Nanostructured Biodegradable Polymer Networks Using Lyotropic Liquid Crystalline Templates

Jason D. Clapper, Stephanie L. Iverson, and C. Allan Guymon*

Chemical and Biochemical Engineering, The University of Iowa, Iowa City, Iowa 52242

Received February 9, 2007; Revised Manuscript Received April 27, 2007

The physical properties, porosity, and physiological behavior of synthetic biodegradable hydrogels have been identified as highly critical design parameters in most tissue engineering materials applications. Nanotechnology may provide the means to manipulate these parameters by accessing control over the network structure of the biomaterial, providing unique property relationships that often result from nanostructured materials. In this study, a lyotropic liquid crystal (LLC) was used as a polymerization template in the formation of a photopolymerizable biodegradable PLA-*b*-PEG-*b*-PLA (PEG = poly(ethylene glycol); PLA = poly(lactic acid)) material with nanoscale lamellar morphology. Through ordering of the biodegradable monomer within the liquid crystal assembly, a 2-fold increase in maximum polymerization rate and a 30% increase in double bond conversion were realized over isotropic monomer formulations. The resulting network structure of the templated PLA-*b*-PEG-*b*-PLA material has a dramatic affect on the physical properties of the hydrogel including an 80% increase in network swelling and an approximately 230% increase in diffusivity. This increase in permeability and solvent uptake leads to rapid degradation of the lamellar templated samples, further demonstrating the influence of the LLC directed network structure on the porosity and physical properties of the biodegradable material. The ability to control the porosity, physical properties, and behavior of a biodegradable hydrogel simply by imparting LLC network structure, without changing the chemistry or biocompatibility of the polymer, could prove highly advantageous in the design of synthetic biomaterials for potential medical applications.

Introduction

The complexity of synthetic polymers developed for tissue engineering applications has grown tremendously over the past decade as researchers continue to identify critical factors and mechanisms that lead to successful and functional tissue growth.[1−5] For example, the ability to correctly tailor the degradation behavior of the scaffold to complement the growth of extracellular matrix is critical in creating space for proliferating cells while still providing the mechanical strength to support the growing tissue.[6,7] Therefore, numerous polymer chemistries have been explored that take advantage of cellular degradation mechanisms, molecular level design, and multicomponent polymer blends toward the precise control over the biodegradation of synthetic tissue constructs.[8−10] In addition, the ability to control the cellular microenvironment within the matrix with features such as high porosity, interconnected pore structure, and biocompatible surface chemistry is necessary for successful tissue function.[11,12] Toward this objective, a variety of techniques have evolved to create 3-D polymer scaffolds with direct control over pore morphology, including methods such as porogen leaching, gas foaming, and colloidal interaction, as well as microfabrication methods such as lithography, negative mold imprinting, and rapid prototyping.[13−19]

In addition to microfabrication, nanoscale fabrication holds tremendous potential in tissue engineering as developed nanotechnology techniques are now being applied to biomaterials in medical applications ranging from nanoscale biosensors to nanoparticle drug carriers.[20−22] Nanostructured biopolymers have the potential to provide many of the critical requirements of tissue scaffolds including precise control over physical properties and a unique cellular environment that may prove favorable over traditionally fabricated biomaterials.[23] Researchers have recently documented enhanced cell attachment with nanoscale scaffold topography,[23−25] as well as superior physical properties with scaffolds incorporating nanofillers such as carbon nanotubes.[26] One of the more successful techniques for the inclusion of nanotechnology in the fabrication of organic polymers is the use of self-assembling media such as lyotropic liquid crystals (LLCs).[27] LLCs possess a number of controllable nanostructured morphologies that have shown promise as polymer templates, directing the growth of 3D polymer matrices with unique network structures.[28−30] A great deal of materials research has focused on the use of LLCs and LLC templated polymers toward applications such as nanoreactors for chemical catalysis,[31] biological sensors,[32] nanoscale selective membranes,[33] and platforms for compatibilizing immiscible monomer mixtures into nanostructured composites.[34]

Although little work has been done toward the fabrication of LLC-structured polymers for tissue engineering applications, previous research has investigated the use of nanostructured LLCs as templates for non-degradable hydrogels.[28,35−38] This work has demonstrated that by simply altering the LLC mesophase geometry of the parent template, the resulting hydrogel network structure can be manipulated, allowing control over the physical properties of the gel that are directly tied to network structure. Since network-based properties such as the water uptake, mechanical properties, and diffusivity/porosity are highly critical properties in tissue engineering materials, it is logical to apply the LLC templating method to biocompatible and biodegradable monomers toward the fabrication of nanostructured synthetic tissue scaffolds.

In this study, multifunctional PLA-*b*-PEG-*b*-PLA (PEG = poly(ethylene glycol); PLA = poly(lactic acid)) biodegradable

* Corresponding author. E-mail: Allan-guymon@uiowa.edu.

10.1021/bm070167l CCC: $37.00
Published on Web 06/14/2007

monomers were photopolymerized within the highly ordered domains of a LLC toward the fabrication of a nanostructured biomaterial. PEG-PLA materials were chosen based on their well-known biocompatibility and biodegradability as a polymer system.[39,40] By studying the phase behavior and interactions between the liquid crystal and biomonomer, as well as the photopolymerization behavior of the monomer within the LLC template, the effects of the parent LLC on the structure of the forming biomaterial matrix were investigated.

It is hypothesized that by inducing a highly ordered mesophase geometry on the network structure of the PLA-*b*-PEG biomaterial, the physical properties such as swelling, modulus, permeability, and degradation may be enhanced and directly controlled. These properties will be measured in two different biodegradable systems in both an isotropic and lamellar LLC templated form. The goal of this study is to use the LLC templating method to manipulate the physical properties and physiological behavior of this biodegradable material without changing its chemistry or biocompatibility. The ability to tailor a single polymer system in this way to meet the many material requirements of a particular tissue engineering application would represent a major advantage in this field.

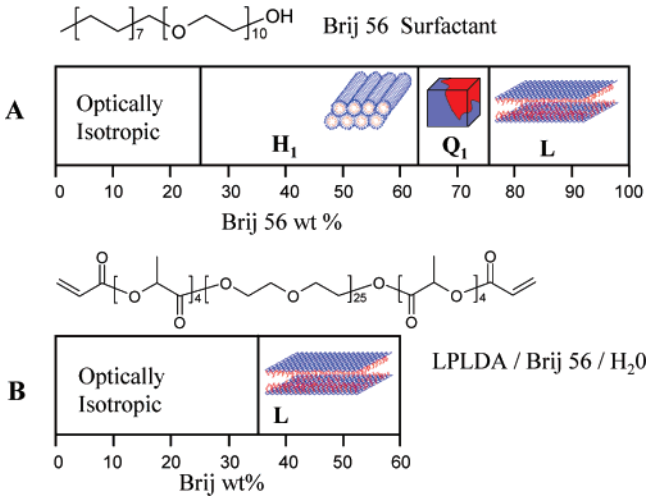

Figure 1. (A) Chemical structure of Brij 56 and phase diagram of Brij 56/water mixtures at 25 °C including figures of LLC morphologies: normal hexagonal (H_1), normal bicontinuous cubic (Q_1), and lamellar (L). (B) Chemical structure of LPL2000-4DA and phase diagram of Brij 56/macromer/water formulations with increasing Brij concentrations.

Experimental Section

Materials. Poly(ethylene glycol) (MWs 2000 and 6000) was obtained from Aldrich and dried via azeotropic distillation with benzene prior to use. Dl-lactide (Polysciences) was recrystallized in hexanes from ethyl acetate. Stannous octoate, polyoxyethylene (10) cetyl ether (Brij 56), and the solute release dyes used in this study, Chicago Sky Blue dye (MW 990) and rhodamine B isothiocyanate-dextran (MW 10 000), were obtained from Aldrich. 1-Hydroxy-cyclohexyl phenyl-ketone (Irgacure 184, Ciba Specialty Chemicals) was used as the radical photoinitiator in all studies.

Synthesis of PLA-*b*-PEG-*b*-PLA Macromers. PLA-*b*-PEG-*b*-PLA macromers were synthesized according to the techniques first described by Sawhney et al. using ring-opening addition of lactide to a central PEG chain followed by capping of the monomer with acrylate or methacrylate functionality.[39] Monomers will follow the notation LPL2000-4DA representing P**L**A-**P**EG-P**L**A (LPL) block configuration with a 2000 MW center PEG chain, four lactide repeat groups on each end of the molecule, and diacrylate (DA) functionality. Dimethacrylated monomers have a similar labeling system with DMA following the lactide number. Four different (meth)acrylated macromers were synthesized including LPL6000-4DA, LPL6000-4DMA, LPL2000-4DA, and LPL2000-4DMA. The chemical structure of LPL2000-4DA is shown in Figure 1. H NMR and infrared spectroscopy were used to confirm the addition of poly(lactide) chains onto the central PEG group with H NMR peaks at 1.5, 4.2, and 5.2 ppm and the growth of the IR peak at 1750 cm^{-1}. The addition of vinyl groups to the macromer was confirmed with H NMR peaks at 5.8, 6.1, and 6.4 ppm and with the appearance of IR peaks at 806 and 1640 cm^{-1}.

Phase Characterization. The optically anisotropic nature of the LLC solutions and those of photopolymerized gels were characterized using a polarized light microscope (PLM, Nikon Eclipse E600W Pol) equipped with a hot stage (Instec, Boulder, CO). Characteristic birefringent light patterns, indicative of the type of order in the LLC mixtures, were used to characterize the morphology of the LLC/macromer system at various Brij 56 concentrations. Samples were prepared by placing approximately 200 μL of LLC/macromer solution between a glass microscope slide and cover slip. Samples were irradiated with a UV source (1.8 mW/cm^2, 10 min) to polymerize the solution. Before and after PLM images were compared and used to determine the degree of disruption in the LLC order that occurs during polymerization.

Small-angle X-ray scattering (SAXS) measurements were taken using a Nonius FR590 X-ray apparatus with a standard copper target Rontgen tube radiation source, a camera, a collimation system of the Kratky type, and a PSD 50M position sensitive linear detector (Hecus M. Braun, Graz). The ratio of the scattering peaks in *d*-spacing was used to determine specific LLC ordered geometry within each sample. In combination with PLM analysis, SAXS profiles were used to characterize the concentration-dependent phase behavior of the LLC/LPL macromer formulations both pre- and post-polymerization, as well as to determine the degree of phase separation between the growing polymer network and the liquid crystal.

Polymerization Analysis. To characterize the photopolymerization of the LLC/LPL macromer blends, isotropic samples with 40 wt % LPL2000-4DA and 60 wt % water, and lamellar templated formulations of 40 wt % LPL2000-4DA, 45 wt % Brij 56, and 15 wt % water were mixed thoroughly at approximately 50 °C. A 0.75 wt % amount of photoinitiator (Irgacure 184) was added to each solution. The photopolymerization reaction was investigated using both photodifferential scanning calorimetry (PDSC) and real-time infrared spectroscopy (RTIR). For PDSC, a Perkin-Elmer differential scanning calorimeter was fitted with a medium-pressure UV arc lamp (ACE Glass) to initiate polymerization. A 365 nm filter was used to control the emission spectrum and light intensity (1.8 mW/cm^2). The polymerization rate profile for both the isotropic- and lamellar templated gels was determined using the exotherm from the polymerization and previously defined methods.[41]

A Thermo Electron Nexus 670 Fourier transform infrared spectrometer was modified to allow for RTIR. Photopolymerization was initiated using a high-pressure Mercury arc lamp (Exfo Acticure 4000) using 365 nm light (1.8 mw/cm^2). The double bond conversion was calculated using the height of the IR peak of the acrylate functional group at 806 cm^{-1} and previously defined methods.[41] Both PDSC and RTIR were conducted at room temperature, allowing the isotropic and lamellar samples adequate time to cool before the tests were conducted.

Physical Property Analysis. Polymer squares were made by pouring 1 mL of either the isotropic or lamellar templated LPL monomer solutions described above into a nylon mold with 2 cm × 2 cm × 0.25 cm troughs. The mold was placed in a nitrogen purged box for 10 min and then irradiated using a 365 nm UV light source (1.8 mW/cm^2, 10 min). Disks were punched from these square polymer samples for both swelling and modulus tests. All disks were soaked in an ethanol solution for 24 h to remove the surfactant and unreacted monomer and then dried overnight in a vacuum oven.

Water uptake was measured gravimetrically by placing the dried polymer disks into 37 °C phosphate-buffered saline (PBS) solution (pH

Table 1. Physical Properties of Templated LPLDMA[a]

monomer	MW	template	water uptake (%)	compressive modulus (kPa)
LPL6000-4DMA	7000	isotropic	920 ± 80	62 ± 6
		lamellar	1580 ± 90	26 ± 6
LPL2000-4DMA	3000	isotropic	200 ± 10	260 ± 40
		lamellar	370 ± 9	150 ± 30

[a] LLC template formulations comprised of 40 wt % LPLDMA with 0 wt % Brij 56 for isotropic samples and 45 wt % Brij 56 for lamellar materials.

7.4). Swelling measurements were taken by removing a disk from solution, patting the surface dry, and recording the mass of the sample. Equilibrium water uptake was determined once the mass of the hydrated sample did not change significantly as a function of overall swell time (approximately 3−5 h) and was calculated using previously defined methods.[36] Dynamic mechanical analysis (DMA, TA instruments Q800 series) was used to determine the compressive modulus of the LLC templated degradable hydrogels. Post-surfactant removal, dehydrated LLC templated hydrogels were incubated in 37 °C PBS solution for 12 h prior to the compressive test to allow the sample to reach equilibrium water uptake but before significant degradation of the gel can occur. Disk-shaped samples were placed on the compressive clamp of the DMA and compressed to approximately 90% of their original thickness. The compressive modulus was calculated using the slope of stress/strain curves from the DMA results. In both the swelling and modulus tests above, three samples of each test material were analyzed to obtain a standard deviation for each resulting data point, represented in Table 1 and by error bars in the reported figures.

Degradation Analysis. The degradation profiles for the LLC templated LPL hydrogels were determined using approximately 50, 1 cm × 1 cm × 0.25 cm squares of each sample material. Degradation studies included LPL2000-4DA formulations with 0 wt % Brij 56 (isotropic), 20 wt % Brij 56 (isotropic), and 45 wt % Brij 56 (lamellar) templates. In addition to surfactant, the formulations comprised of 40 wt % LPL2000-4DA macromer, water, and 0.75 wt % photoinitiator. In addition, sets of LPL6000-4DA of either isotropic (0 wt % Brij 56) or lamellar (45 wt % Brij 56) structure were analyzed to study the degradation of this material in templated and nontemplated form. For the degradation runs, dried squares of each sample were initially weighed and immersed in approximately 20 mL of PBS solution in individual vials kept at 37 °C. Samples were removed at designated times and weighed in both the hydrated and dried state. In addition, on predesignated dates, triplicate samples were removed to gauge the variability in the degrading samples, represented by error bars on the mass loss and water uptake figures. Mass loss and water uptake were recorded as a function of time. The pH of the sample solutions was also tracked; and if one particular solution registered a pH of lower than 6.5, all vials for that material were replenished with new PBS solution.

Diffusion Analysis. Three 1 cm × 1 cm × 0.25 cm squares of both lamellar and isotropic templated LPL2000-4DMA were dehydrated post-surfactant removal and soaked in aqueous solutions of Chicago Sky Blue dye (0.5 mg/mL) or rhodamine B isothiocyanate-dextran (11 mg/mL) for 3 weeks to allow complete saturation of the dye. A 1% (w/v) amount of citric acid was added to the aqueous soak solutions, bringing the pH to approximately 2.2 to prevent degradation. After 2 weeks, the gels were removed, rinsed thoroughly, and placed in the upper chamber of a spectra cell containing approximately 2.5 mL of distilled water with adjusted pH (~2.2). The gels were restricted from the lower half of the spectra cell where UV visible spectrometry readings at 614 and 560 nm were performed for the Chicago Sky Blue dye and rhodamine B isothiocyanate-dextran, respectively.

Results and Discussion

Numerous studies have investigated the effects of using LLC templates on non-degradable polymer systems, examining the relationships between the LLC morphology and the polymerization kinetics,[38,42,43] the network structure,[28,35] and the physical properties of the LLC structured materials.[28,36,37] It was found that by controlling the network structure of a polymer through LLC templating, the physical properties of the material can be directly manipulated.[36,37] The current study investigates the effects of templating a biodegradable polymer system, PLA-*b*-PEG-*b*-PLA with a highly ordered lamellar LLC, a method of polymer processing on the nanoscale that has not been seen in the biodegradable polymer field. To explore the relationships between the induced lamellar network structure and the properties of the gel, the templated LLC phase behavior, photopolymerization behavior, network swelling, modulus, permeability, and degradation behavior were all investigated for both LLC lamellar and traditional isotropic forms of the biodegradable polymer matrix.

Phase Behavior and Structure Retention. Formulations of Brij 56 surfactant and water exhibit a number of LLC phase morphologies that possess highly ordered nanoscale geometric structures. Figure 1A shows the chemical structure of Brij 56 as well as a phase diagram of Brij 56 and water at 25 °C, as determined in previous studies.[44] Type 1 or normal hexagonal and normal bicontinuous cubic LLC mesophases are generated in addition to the lamellar LLC mesophase. Earlier work in our laboratory has shown that the addition of a third component, a photopolymerizable monomer, often changes the phase behavior and mesophase transition boundaries of Brij 56/water mixtures by acting as a co-surfactant.[35,37] This phase changing behavior is also observed as the PLA-*b*-PEG-*b*-PLA macromer is added to the Brij 56/water system. Figure 1B demonstrates that additions of LPL macromer inhibit the formation of normal hexagonal (H_1) and normal bicontinuous cubic (Q_1) phases, with only the lamellar phase (L) forming above surfactant concentrations of 35 wt %. It is hypothesized that the large hydrophilic LPL macromers limit the formation of the curved geometries of the hexagonal and cubic phases, leaving the lamellar phase as the most entropically favorable morphology even at relatively low concentrations of Brij 56. The large downward shift in the Brij 56 concentration limit for the lamellar phase, from 74 wt % in the binary system to 30 wt % in the formulations with added LPL macromer, is also a direct result of the degradable macromer in the LLC system. In this case, the 40 wt % of LPL macromer acts not only as a co-surfactant to the Brij 56 but also serves to limit the amount of water in the formulation, increasing the concentration of Brij 56 relative to water, further lowering the necessary surfactant concentration to form the lamellar LLC.

The morphology of the polymer structure generated from LLC templating has been the focus of a great deal of recent interest in the formation of nanostructured materials. Studies have demonstrated that the type of monomer chemistry/functionality, the type of surfactant used, and the polymerization kinetics all play a significant role in the LLC templating process, resulting in polymer networks that range from an obvious copy of the parent LLC template to polymer structures that are phase-separated from the liquid crystal.[28−30,45] In this work, SAXS and polarized light microscopy PLM were used to probe the lamellar templated hydrogels before and after photopolymerization for evidence of phase retention and lamellar morphology. PLM images of 40 wt % LPL6000-4DA or LPL2000-4DA with 40 wt % Brij 56 (lamellar), before and after photopolymerization, were very similar, suggesting that the polymerization of the LPL macromers in each case did not significantly disrupt the lamellar morphology, resulting in a polymer network

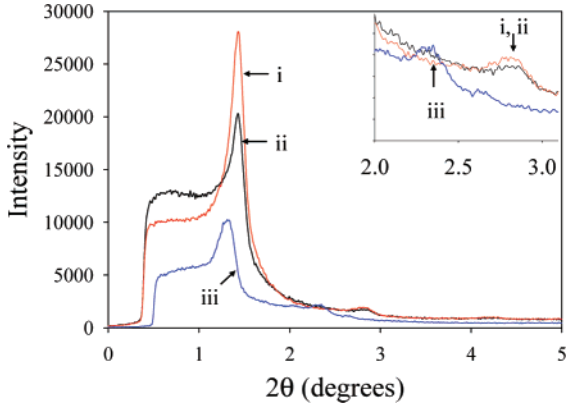

Figure 2. SAXS profiles for lamellar LLC mixtures of 40 wt % LPL2000-4DMA, 40 wt % Brij 56, and 20 wt % water both pre-polymerization (lamellar) (i) and post-polymerization (lamellar) (ii), as well as a Brij/water mixture (hexagonal) (iii) with the same surfactant to water ratio as in the polymerized sample. Inset shows the secondary scattering peaks for the three profiles.

structure that is very similar to the parent LLC template. Due to the high degree of cross-linking in the LPLDMA material, we do not expect the lamellar morphology to be disrupted upon removal of the surfactant. Recent work in our laboratory has shown that for highly cross-linking (meth)acrylate monomers, the anisotropic nature of the templated system is often retained even after surfactant removal from the polymer.

SAXS profiles of the 40 wt % Brij and 40 wt % LPL macromer formulations demonstrated nanostructured lamellar ordering in the LLC/LPL systems, both before and after polymerization. Figure 2 shows (i) pre- and (ii) post-polymerization SAXS profiles for a lamellar formulation of 40 wt % LPL2000-4DMA. In Figure 2, it is observed that the intensity of the primary scattering peak decreases upon polymerization due to the change of the liquid monomer to solid polymer. However, the spacing of primary and secondary scattering peaks upon polymerization does not change, indicating very little disruption in the spacing of the lamellar layers. Figure 2iii also shows the SAXS profile for a 2:1 Brij:water system, equivalent to the ratio of surfactant to water that would be present in the lamellar templated material if the polymer completely phase-separated from the LLC and did not interact with the surfactant system. In the surfactant/water profile, the primary and secondary peaks are lower in intensity compared to that of the polymerized ternary system. Furthermore, the spacing ratio for the primary to secondary peak in the Brij/water system is characteristic of hexagonal ordering. The fact that the post-polymerization SAXS profile of the LPLDMA system retains the lamellar scattering pattern and does not shift to a hexagonal profile is highly indicative that the lamellar morphology of the parent template is retained in the resulting polymer network with little to no phase separation from the LLC.

Polymerization Characterization. The polymerization rate and conversion of monomer are highly affected by the LLC geometry used to template the forming polymer networks in LLC systems.[38,42,43] To explore the effects of polymerizing the PLA-*b*-PEG-*b*-PLA macromers within the highly ordered domains of the lamellar LLC, photo-differential scanning calorimetry (PDSC) and RTIR were used to investigate the polymerization of isotropic and lamellar templated LPL2000-4DA formulations. Figure 3 shows the polymerization exotherms taken using PDSC as well as the conversion profiles observed using RTIR for LPL2000-4DA. The diacrylate version of the PLA-*b*-PEG-*b*-PLA macromer was used in the polymerization studies due to its rapid polymerization rate compared to

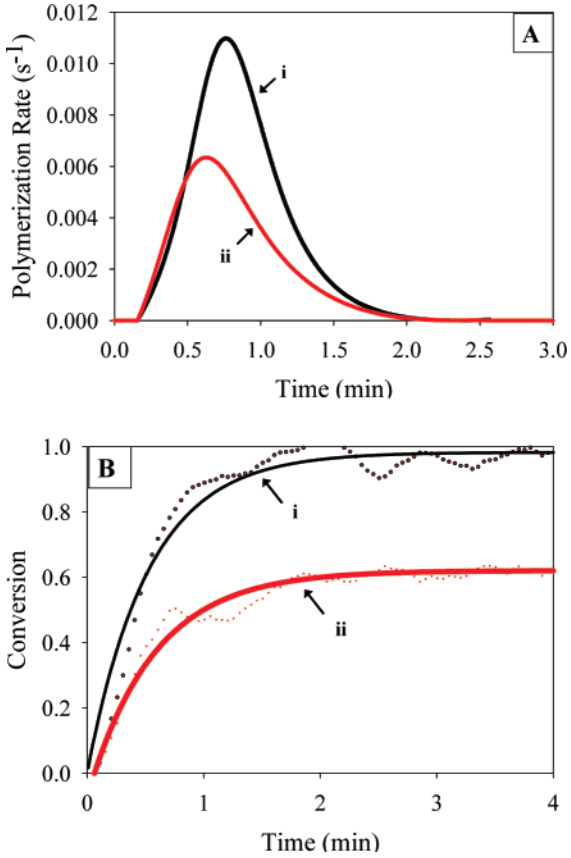

Figure 3. (A) P-DSC polymerization profiles describing the rate of polymerization vs time and (B) RTIR profiles showing the double bond conversion vs time of 40 wt % LPL2000-4DA in both lamellar (i) and isotropic (ii) formulations. All polymerizations were initiated with UV irradiation at time 0.

methacrylated macromers, yielding more prominent and reproducible DSC exotherms for the analysis of templating effects on polymerization behavior. Figure 3A demonstrates that the LPL2000-4DA macromer photopolymerized within the lamellar template (40 wt % Brij 56) exhibits a maximum polymerization rate that is approximately 80% higher than the same monomer polymerized in an isotropic state (0% Brij 56). Similarly, Figure 3B shows a significant increase in polymerization rate with the LPL macromer that is polymerized in the lamellar template, as well as approximately 30% more acrylate double bond conversion in this system when compared to the same macromer polymerized in an isotropic state.

The observed increase in rate and conversion is the result of the close association between the LPL degradable monomer and the liquid crystal leading to the segregation of monomer into the nanoscale domains of the LLC template. The combined effects of an increase in local monomer concentration, limited mobility of the growing polymer chains, and decreased termination effects serve to increase both the observed rate of polymerization in the lamellar system as well as increase the degree of conversion in the templated network.[42,43] There are many advantages, from a tissue scaffold standpoint, that result from polymer networks with a high degree of conversion, including increased biocompatibility with less unreacted monomer in the network, as well as increased mechanical properties with high degrees of conversion and cross-linking.[46]

Swelling and Mechanical Properties of Templated Materials. The initial degree of water uptake and mechanical properties of templated PLA-*b*-PEG-*b*-PLA materials were investigated

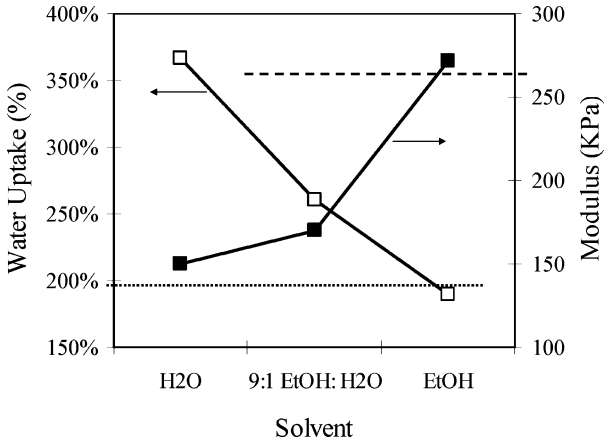

Figure 4. Solvent uptake (□) and compressive modulus (■) of lamellar templated LPL2000-4DMA placed in solvents with increasing ethanol concentration. The upper and lower horizontal lines represent the compressive modulus (--) and degree of solvent uptake (···) respectively of water-swollen isotropic LPL2000-4DMA.

to determine if the physical properties of a biodegradable hydrogel can be manipulated simply by changing the nanostructured LLC template used to create the gel. In this study, swelling and modulus tests were conducted on templated and isotropic, LPL6000-4DMA and LPL2000-4DMA networks. By removing all of the surfactant from these gels post-polymerization, the isotropic and lamellar-structured degradable networks are chemically and compositionally equivalent, allowing for direct observations to be made between the network structure of the gels and their resulting physical properties. Table 1 lists the degree of water uptake as well as the compressive modulus of isotropic and lamellar templated LPLDMA materials. As the molecular weight of the PEG block in the macromer is changed from 6000 to 2000, which increases the overall cross-linking density in the resulting network, the equilibrium swelling of both the isotropic and lamellar gels decreases on average nearly 360%, while the compressive modulus increases approximately 330%.

Alternatively, within one monomer molecular weight, the physical properties of the gel can be manipulated simply by templating the network with the lamellar LLC. Table 1 shows a 70% increase in swelling and 55% decrease in the modulus of lamellar templated LPL6000-4DMA when compared to the isotropic network of the same macromer. Similarly with LPL2000-4DMA, an 80% increase in swelling and 45% decrease in modulus results in the lamellar templated network compared to the material polymerized in an isotropic state. The large, continuous pores resulting from the LLC template have been documented to increase the swelling and porosity of non-degradable polymers templated with highly ordered hexagonal and lamellar LLC morphologies, as is the case here with the lamellar templated biodegradable PLA-*b*-PEG-*b*-PLA.[37]

In traditional hydrogel systems, the modulus of the gel is often inversely related to the degree of water uptake in the network due to the decrease in cross-link density that occurs as these gels become highly swollen.[47] To determine if the increased water uptake in the lamellar templated gels is responsible for the observed decrease in modulus (Table 1), lamellar templated dehydrated LPL2000-4DMA samples were placed in aqueous solutions with increasing concentration of ethanol to limit the overall swell of these gels. Figure 4 shows the degree of solvent uptake and compressive modulus of lamellar templated LPL2000-4DMA as the gel is placed in three solvents (pure water, a 9:1 water−ethanol mix, and pure ethanol), as well as the water uptake and modulus for the isotropic LPL2000-4DMA.

As the ethanol concentration in the solvent is increased, the swelling of the lamellar templated LPLDMA decreases (Figure 4). When the solvent is 100% ethanol, the swelling of the lamellar templated material is approximately equal to the degree of solvent uptake in the water-swollen isotropic sample (200%). Looking at the compressive modulus of the lamellar templated ethanol-swollen material, the compressive modulus is approximately equal to that of the isotropic sample swelled in water (265 KPa). Therefore, by making the lamellar and isotropic templated LPLDMA materials swell to the same degree, we see that the modulus of the two materials is also equal. This result suggests that the drop in modulus for the lamellar templated hydrogel in water is primarily due to the increase in water uptake in the system, and not due to a detrimental change in the network integrity of the gel from the lamellar template.

Degradation of Templated Materials. The amount of water in a swollen biodegradable hydrogel is one of the main factors governing the rate of degradation as the hydrolysis of ester bonds in PLA-*b*-PEG-*b*-PLA materials is the primary mechanism of gel degradation.[48] Due to the ability to manipulate the degree of water uptake in the degradable LPLDMA gels simply by changing the parent LLC template used to create the gel, this study investigated the influence of LLC templating on the degradation kinetics of the biodegradable material. Toward this end, LPL6000-4DMA and LPL2000-4DMA in both the isotropic and lamellar form were analyzed as they degraded in 37 °C PBS solution. Transient swelling was also tracked for the isotropic and lamellar LPLDMA materials as this property is directly related to degradation. Figure 5 shows the degradation profiles and transient swelling profiles for LPL2000-4DMA in isotropic (0 wt % Brij 56) and lamellar (45 wt % Brij 56) form. LPL2000-4DMA fabricated with a 20 wt % Brij 56 template was also investigated, although this specific surfactant concentration does not yield a highly ordered LLC phase and is optically isotropic in nature. Similar to the property testing above, removing the surfactant from all gels prior to degradation renders these materials chemically and compositionally equivalent, suggesting that the observed property differences are solely due to the lamellar template imposed on the biodegradable hydrogel's network.

In Figure 5A, it is observed that both isotropic gels degrade in a similar manner even though one of the gels was fabricated with the 20 wt % surfactant template. In comparing the isotropic gels to the lamellar templated PLA-*b*-PEG-*b*-PLA materials, however, the LLC templated gel exhibits a much greater initial degradation rate, losing almost 40% of its mass within the first 10 days of degradation. The greater initial degradation rate of the lamellar templated network is directly related to the increased water uptake in the LLC hydrogel, an 80% increase over the isotropic hydrogel of the same material. Increased swelling will not only bring more water into the network, cleaving more hydrolyzable bonds in the process, but will also greatly increase the porosity of the gel, leading to a greater diffusion of degradation products and release of structures such as cyclic chains that are not tethered to the network. It is also observed that when all three of the networks become sufficiently swollen (day 10, Figure 5A), the rate of degradation is approximately equal between the materials as the chemistry and concentration of the polymer cross-links (equivalent in all cases), not the water uptake, become the dominant factors in the degradation rate of these materials.

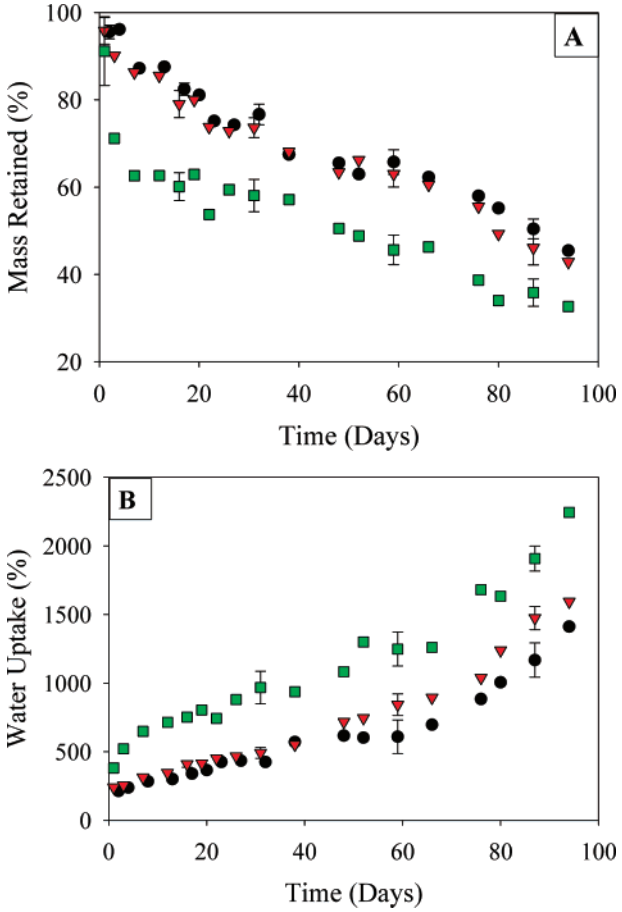

Figure 5. (A) Degradation profiles and (B) transient swelling profiles of 40 wt % LPL2000-4DMA templated with 0 wt % Brij 56 (isotropic) (●), 20 wt % Brij 56 (isotropic) (▼), and 45 wt % Brij 56 (lamellar) (■).

The increased porosity and water uptake for the lamellar templated LPLDMA material is also demonstrated in Figure 5B. Again, the transient water uptake profiles for both isotropic samples are very similar throughout the degradation of both materials. However, the lamellar templated biodegradable hydrogel exhibits a rapid initial increase in water uptake over the isotropic samples that, in turn, greatly influences the degradation of the lamellar gel as mentioned above. Though the results are not shown here, the degradation and transient swelling for the larger LPL6000-4DMA hydrogels were very similar to the LPL2000-4DMA results in Figure 5. The lamellar templated LPL6000-4DMA consistently swells to almost twice the degree of the isotropic sample throughout the degradation, and, consequently, the lamellar sample degraded in approximately 60% of the time required by the isotropic samples. Thus in both LPLDMA systems, by simply changing the structure of the material through the use of a nanostructured LLC template, significant control over the degradation of the biodegradable materials is realized.

In addition, it is often advantageous in tissue engineering applications to have a material that exhibits the rapid initial mass loss observed in the degradation profile of lamellar templated gel (Figure 5). This type of degradation will rapidly increase the porosity of the gel, allowing cells a favorable environment of excess water and nutrient diffusion, while still retaining much of the polymer's network and thus its mechanical strength.[7,19] Typically, to increase degradation and maximize porosity in PLA-*b*-PEG-*b*-PLA samples, a decreased macromer concentration or a larger macromer size is used in an effort to decrease

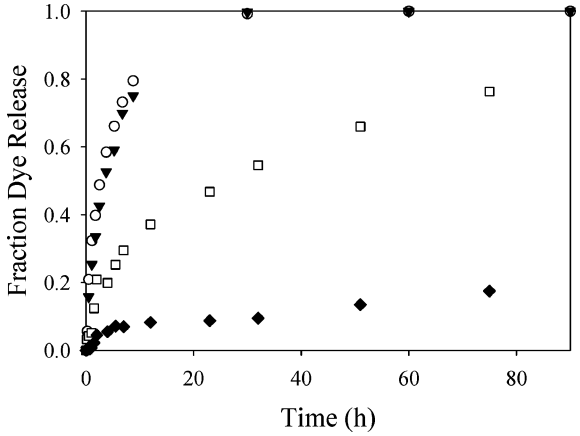

Figure 6. Release profiles for Chicago Sky Blue dye from lamellar- (○) and isotropic (▼) templated 40 wt % LPL2000-4DMA, as well as release profiles of rhodamine B isothiocyanate-dextran from lamellar (□) and isotropic (◆) templated 40 wt % LPL2000-4DMA.

cross-linking density, often at the expense of mechanical properties. However, the results above demonstrate that the lamellar templated LPLDMA gels exhibit a more rapid initial degradation and water uptake over isotropic samples even though they have approximately 30% more conversion in these systems (Figure 3), a result that does not indicate a decrease in cross-link density for the templated hydrogel.

Permeability Analysis of Templated PLA-*b*-PEG-*b*-PLA

As stated above, the LLC water domains in the lamellar templated LPLDMA hydrogels are thought to increase the water uptake and permeability of these gels, leading to a higher degree of swelling, greater porosity, and a faster degradation when compared to isotropic networks made of the same material. To directly probe the permeability or diffusivity of the templated PLA-*b*-PEG-*b*-PLA degradable gels, small molecular weight solutes were loaded into both lamellar templated and isotropic LPL2000-4DMA swollen hydrogels. This process was performed after surfactant removal by swelling each gel in a saturated aqueous solution of the dye, allowing the solute to infiltrate the pores of the hydrogel construct. To minimize degradation effects from the LPLDMA polymer during the solute release tests, all solutions were modified with 1% (w/v) citric acid to bring the pH to approximately 2.2, a level at which little to no hydrolysis occurs and the networks do not degrade. The swelling or water uptake of the templated or isotropic LPLDMA gels did not change significantly as the pH was lowered to 2.2, and thus we do not expect significant structural changes to the gel as a result of this low pH for solute release analysis.

Figure 6 shows the release profiles of two different molecular weight dyes from both lamellar templated and isotropic LPL2000-4DMA. With the smaller Chicago Sky Blue dye (MW 990), we see that the lamellar and isotropic samples both release the dye rapidly with no apparent difference in network diffusivity. The high degree of swelling and porous network structure of the LPL hydrogels does not hinder the transport of the small dye molecules from either the templated or isotropic material, making the expected increase in permeability in the lamellar LLC material undetectable.

Using a larger molecular weight dye, rhodamine B isothiocyanate-dextran (MW 10 000), a significant variance in the release profiles between the lamellar and isotropic samples is observed (Figure 6). The larger rhodamine dye is released much more slowly from the isotropic gel than the lamellar templated degradable hydrogel. Disregarding the first 10 h of each release

profile to minimize the burst release effects of dye on the surface of the gel, the slope of both the templated and isotropic release profiles for rhodamine dye was analyzed. The templated LPL2000-4DMA releases the larger molecular weight dye at an approximate rate of 0.5%/h, a rate that is over double that of the isotropic gel at 0.21%/h. This increase in permeability is brought about by the long-range continuous pores that result from the lamellar template, whereas in the isotropic material, the diffusing dye has a much more tortuous path. Furthermore, the increased permeability in the LLC templated LPLDMA, allowing for greater water uptake and increased diffusion of degradation products, is most likely accountable for the initial rapid degradation observed for the lamellar templated hydrogels.

In the permeability investigation above and all investigations of this study, the surfactant of the LLC template was removed from the hydrogels before testing to ensure that the diffusivity variances observed can be solely attributed to the altered network structure of the lamellar templated LPLDMA. Due to the fact that the lamellar and isotropic polymers are chemically equivalent and made with the same macromer content in solution, the change in properties for the lamellar templated LPLDMA can be directly attributed to its network structural arrangement, an immediate function of the parent lamellar template used to create the degradable hydrogel. Thus, simply by controlling the network structure of the PLA-*b*-PEG-*b*-PLA hydrogel using the liquid crystal template, significant enhancements were made not only to the polymerization behavior of the degradable material, but also to critical scaffold characteristics such as water uptake, degradation behavior, and permeability. Finally, using the lamellar nanostructured LLC as a polymerization template allowed for the manipulation of the physical properties of a biomaterial without changing the chemistry or general biocompatibility of the biopolymer.

Conclusions

In this study, a lamellar LLC template was used to create a nanostructured cross-linked biodegradable PLA-*b*-PEG-*b*-PLA hydrogel. This process leads to significant changes in the photopolymerization behavior, the structure of the network, and its physical behavior when compared to the isotropic form of the same material. By ordering the degradable macromers within a lamellar liquid crystal, an 80% enhancement in polymerization rate and 30% greater acrylate double bond conversion is attained. The lamellar-structured network also exhibits increases in initial swelling and permeability of 75 and 230%, respectively, when compared to traditional isotropic PLA-*b*-PEG-*b*-PLA samples. This increase in water swelling and permeability directly leads to a more rapid degradation of the lamellar templated hydrogel compared to isotropic materials of the same chemistry and composition. Finally, the LLC templating technique was demonstrated as a simple processing method that serves to control the swelling, porosity, and most importantly the degradation profile of a biodegradable polymer without changing the chemistry or composition of that gel, a significant advancement for biodegradable polymers for biomedical applications.

Acknowledgment. The authors gratefully acknowledge financial support from The University of Iowa through a Biosciences Initiative Grant and Presidential Fellowship, and from The National Science Foundation (Grants PECASE CBET0328231 and CBET0626395)

References and Notes

(1) Niklason, L. E., Gao, J.; Abbott, W. M.; Hirschi, K. K.; Houser, S.; Marini, R.; Langer, R. *Science* **1999**, *284*, 489−493.
(2) Chastain, S. R.; Kundu, A. K.; Dhar, S.; Calvert, J. W.; Putnam, A. J. *J. Biomed. Mat. Res.* **2006**, *78A*, 73−85.
(3) Tan, W.; Krishnaraj, R.; Desai, T. A. *Tissue Eng.* **2001**, *7*, 203−210.
(4) Bryant, S. J.; Anseth, K. S.; Lee, D. A.; Bader, D. L. *J. Orthod. Res.* **2004**, *22*, 1143−1149.
(5) Hacker, M. C.; Mikos, A. G. *Tissue Eng.* **2006**, *12*, 2049−2057.
(6) Drury, J. L.; Mooney, D. J. *Biomaterials* **2003**, *24*, 4337−4351.
(7) Bryant, S. J.; Bender, R. J.; Durand, K. L.; Anseth, K. S. *Biotechnol. Bioeng.* **2004**, *7*, 747−755.
(8) Burdick, J. A.; Chung, C.; Jia, X.; Randolph, M. A.; Langer, R. *Biomacromolecules* **2005**, *6*, 386−391.
(9) Rydholm, A. E.; Reddy, S. K.; Anseth, K. S.; Bowman, C. N. *Biomacromolecules* **2006**, *7*, 2827−2836.
(10) Benoit, D. S. W.; Durney, A. R.; Anseth, K. S. *Tissue Eng.* **2006**, *7*, 1663−1673.
(11) Moon, J. J.; Lee, S. H.; West, J. L. *Biomacromolecules* **2007**, *8*, 42−49.
(12) Shin, H.; Jo, S.; Mikos, A. G. *Biomaterials* **2003**, 24, 4353−4364.
(13) Mi, Y.; Chan, Y.; Trau, D.; Huang, P.; Chen, E. *Polymer* **2006**, *47*, 5124−5130.
(14) Xie, B.; Parkhill, R. L.; Warren, W. L.; Smay, J. E. *Adv. Funct. Mater.* **2006**, *16*, 1685−1693.
(15) Shum, A. W. T.; Li, J.; Mak, A. F. T. *Polym. Degrad. Stab.* **2005**, *87*, 487−493.
(16) Mahmood, T. A.; Shastri, V. P.; Van Blitterswijk, C. A.; Langer, R.; Riesle, J. *Tissue Eng.* **2005**, *11*, 1244−1253.
(17) Pfister, P. M.; Wendlandt, M.; Neuenschwander, P.; Suter, U. W. *Biomaterials* **2007**, *28*, 567−575.
(18) Sarkar, S.; Lee, G. Y.; Wong, J. Y.; Desai, T. A. *Biomaterials* **2006**, *27*, 4775−4782.
(19) Landers, R.; Hubner, U.; Schmelzeisen, R.; Mulhaupt, R. *Biomaterials* **2002**, *23*, 4437−4447.
(20) Peppas, N. A.; Hilt, J. Z.; Khademhosseini, A.; Langer, R. *Adv. Mater.* **2006**, *18*, 1345−1360.
(21) Yih, T. C.; Al-Fandi, M. *J. Cell Biochem.* **2006**, *97*, 1184−1190.
(22) Farokhzad, O. C.; Langer, R. *Adv. Drug. Delivery Rev.* **2006**, *58*, 1456−1459.
(23) Pham, Q. P.; Sharma, U.; Mikos, A. G. *Tissue Eng.* **2006**, 12, 1197−1211.
(24) Price, R. L.; Haberstroh, K. M.; Webster, T. J. *Nanotechnology* **2004**, *15*, 892−900.
(25) Rajagopalan, P.; Shen, C. J.; Berthiaume, F.; Tilles, A. W.; Toner, M.; Yarmush, M. L. *Tissue Eng.* **2006**, *12*, 1553−1563.
(26) Koyama, S.; Haniu, H.; Osaka, K.; Koyama, H.; Kuriowa, N.; Endo, M.; Kim, Y. A.; Hayashi, T. *Small* **2006**, *2*, 1406−1411.
(27) Hentze, H. P.; Kaler, E. W. *Curr. Opin. Colloid Interface Sci.* **2003**, *8*, 164−178.
(28) DePierro, M. A.; Carpenter, K. G.; Guymon, C. A. *Chem. Mater.* **2006**, *18*, 5609−5617.
(29) Wadekar, M. N.; Pasricha, R.; Gaikwad, A. B.; Kumaraswamy, G. *Chem. Mater.* **2005**, *17*, 2460−2465.
(30) Anderson, D. M.; Strom, P. *Physica A* **1991**, *176*, 151−167.
(31) Gin, D. L.; Gu, W.; Pindzola, B. A.; Zhou, W.-J. *Acc. Chem. Res.* **2001**, *34*, 973−980.
(32) Van Nelson, J. A.; Kim, S. R.; Abbott, N. L. *Langmuir* **2002**, *18*, 5031−5035.
(33) Zhou, M.; Kidd, T. J.; Noble, R. D.; Gin, D. L. *Adv. Mater.* **2005**, *17*, 1850−1853.
(34) Clapper, J. D.; Guymon, C. A. *Adv. Mater.* **2006**, *18*, 1575−1580.
(35) McCormick, D. T.; Stovall, K. D.; Guymon, C. A. *Macromolecules* **2003**, *36*, 6549−6558.
(36) Lester, C. L.; Smith, S. M.; Colson, C. D.; Guymon, C. A. *Chem. Mater.* **2003**, *15*, 3376−3384.
(37) Clapper, J. D.; Guymon, C. A. *Macromolecules* **2007**, *40*, 1101−1107.
(38) Lester, C. L.; Smith, S. M.; Jarrett, W. L.; Guymon, C. A. *Langmuir* **2003**, *19*, 9466−9472.
(39) Sawhney, A. S.; Pathak, C. P.; Hubbell, J. A. *Macromolecules* **1993**, *26*, 581−587.
(40) Metters, A. T.; Anseth, K. S.; Bowman, C. N. *Polymer* **2000**, *41*, 3993−4004.
(41) White, T. J.; Liechty, W. B.; Natarajan, L. V.; Tondiglia, V. P.; Bunning, T. J.; Guymon, C. A. *Polymer* **2006**, *47*, 2289−2298.

(42) DePierro, M. A.; Guymon, C. A. *Macromolecules* **2006**, *39*, 617−626.
(43) Lester, C. L.; Smith, S. M.; Guymon, C. A. *Macromolecules* **2001**, *34*, 8587−8589.
(44) Coleman, N. R. B.; Attard, G. S. *Microporous Mesoporous Mater.* **2001**, *44*, 73−80.
(45) Antonietti, M.; Caruso, R. A.; Goltner, C. G.; Weissenberger, M. C. *Macromolecules* **1999**, *32*, 1383−1389.
(46) Sabino, M. A.; Ajami, D.; Salih, V.; Nazhat, S. N.; Vargas-Coronado, R.; Cauich-Rodriguez, J. V.; Ginebra, M. P. *J. Biomater. Appl.* **2004**, *19*, 147−161.
(47) Perera, D. I.; Shanks, R. A. *Polym. Int.* **1996**, *39*, 121−127.
(48) Von Burkersroda, F.; Schedl, L.; Gopferich, A. *Biomaterials* **2002**, *23*, 4221−4231.

BM070167L